FEBS Letters

FEBS PRESS science publishing by scientists

REVIEW

Biological nitrogen fixation in theory, practice, and reality: a perspective on the molybdenum nitrogenase system

Stephanie D. Threatt and Douglas C. Rees

Division of Chemistry and Chemical Engineering, Howard Hughes Medical Institute, California Institute of Technology, Pasadena, CA, USA

Correspondence
D. C. Rees, Division of Chemistry and Chemical Engineering, 147-75, Howard Hughes Medical Institute, California Institute of Technology, Pasadena, CA 91125, USA
Tel: 1-626-395-8393
E-mail: dcrees@caltech.edu

(Received 4 October 2022, revised 30 October 2022, accepted 31 October 2022, available online 28 November 2022)

doi:10.1002/1873-3468.14534

Edited by Martin Högbom

Nitrogenase is the sole enzyme responsible for the ATP-dependent conversion of atmospheric dinitrogen into the bioavailable form of ammonia (NH_3), making this protein essential for the maintenance of the nitrogen cycle and thus life itself. Despite the widespread use of the Haber–Bosch process to industrially produce NH_3, biological nitrogen fixation still accounts for half of the bioavailable nitrogen on Earth. An important feature of nitrogenase is that it operates under physiological conditions, where the equilibrium strongly favours ammonia production. This biological, multielectron reduction is a complex catalytic reaction that has perplexed scientists for decades. In this review, we explore the current understanding of the molybdenum nitrogenase system based on experimental and computational research, as well as the limitations of the crystallographic, spectroscopic, and computational techniques employed. Finally, essential outstanding questions regarding the nitrogenase system will be highlighted alongside suggestions for future experimental and computational work to elucidate this essential yet elusive process.

Conversion of dinitrogen (N_2) to the fixed form of ammonia (NH_3) is essential for life, as fixed nitrogen is a key component of many biological molecules [1,2]. Inert N_2 is abundant, as it represents ~ 80% of Earth's atmosphere; however, this N–N triple bond represents one of the strongest bonds in nature [3] and often requires complex transition metal systems to promote nitrogen reduction. Namely, the industrial Haber–Bosch process and biological N_2 fixation by nitrogenase (N_2ase), which both feature multiple Fe centres, are responsible for generating nearly all of the bioavailable nitrogen on our planet. While the Haber–Bosch process represents a significant industrial advancement that has supported an increase of ~ 6 billion people in the global population over the past century, it requires high temperatures and pressures for catalysis and currently consumes approximately 2% of the world's annual energy production, while accounting for 1.4% of global carbon dioxide (CO_2) emissions [4–7]. By contrast, the biological process naturally operates under physiological conditions, where the equilibrium strongly favours ammonia production. Given the efficiency with which nitrogenase performs the catalytic conversion of N_2 to NH_3, there has been considerable research focused towards understanding the catalytic strategy employed for biological nitrogen reduction.

Biological nitrogen fixation is catalysed by the enzyme nitrogenase that naturally exists as three isozymes: Mo-nitrogenase, V-nitrogenase, and Fe-nitrogenase, which contain different coordinating metals within their active site metallocofactors (molybdenum, vanadium, and iron, respectively) [8–14]. Most studies have focused on the molybdenum-variant of nitrogenase (Mo-N_2ase), which has been well-characterized and displays the greatest catalytic activity. The stoichiometry of the Mo-N_2ase reduction reaction is typically represented as follows:

$$N_2 + 8\,H^+ + 8\,e^- + 16\,MgATP \rightarrow 2\,NH_3 + H_2 + 16\,MgADP + 16\,P_i,$$

Abbreviations
ATP, adenosine triphosphate; DF, density functional; EPR, electron paramagnetic resonance; Fe protein, iron protein; FeMoCo, iron molybdenum cofactor; MoFe protein, molybdenum iron protein; N_2, dinitrogen; N_2ase, nitrogenase; NH_3, ammonia.

This is an open access article under the terms of the Creative Commons Attribution License, which permits use, distribution and reproduction in any medium, provided the original work is properly cited.

with obligatory hydrogen (H_2) evolution accompanying N_2 reduction. While nitrogenase utilizes ecologically friendly energy sources as reducing equivalents, the Mo-N_2ase requirement for 16 MgATP molecules highlights that both the biological and industrial processes are energy consumptive. In contrast to the biological process that operates under ambient conditions, Haber–Bosch plants require high pressures between 200 and 400 atm and temperatures of 500 °C alongside notable methane consumption to source hydrogen, making the industrial process very energy intensive, as well as a potent source of greenhouse gas emissions [5]. Given the need for more efficient and sustainable strategies for large-scale NH_3 production, there have been decades of research dedicated to understanding the N_2ase system. Studies of the Mo-N_2ase, V-N_2ase, and Fe-N_2ase systems have revealed structural and electronic similarities for all isoforms that support a universal, eight-electron mechanism for N_2 reduction by these N_2ases [9,11,12,15]; however, slight differences in the cofactor and surrounding protein scaffold between isoforms have provided unique insights about the general reduction mechanism. Importantly, many mechanistic details of the catalytic strategy employed by nitrogenase to successfully lower the activation barrier for N_2 reduction relative to the industrial process remain enigmatic [16]; however, further understanding of the biological nitrogen reduction mechanism is essential for the development of more efficient catalysts for ammonia production that operate under mild reaction conditions while also being more sustainable.

This review will focus mainly on experimental characterizations of the Mo-N_2ase system, which have been aided by advances in spectroscopy and crystallography, as well as recent computational studies that have provided further insights into the role of various active site features and produced hypotheses for potential catalytic mechanisms (note, a 2020 review by Jasniewski et al. covers studies of the Fe- and V-N_2ase systems [11]). The limitations of both experimental and computational investigations of nitrogenase will then be described, followed by outstanding mechanistic questions. Lastly, recent developments with the potential to further elucidate this complex and essential catalytic process will be discussed.

Experimental insights into biological nitrogen fixation

The well-studied Mo-N_2ase system [8–10,12] consists of two-component metalloproteins that together catalyse the ATP-dependent conversion of N_2 to NH_3: the molybdenum iron (MoFe) protein and the iron (Fe) protein. MoFe protein is an $\alpha_2\beta_2$ tetramer that contains two metalloclusters, specifically an [8Fe:7S] P cluster and a [7Fe:9S:C:Mo]-*R*-homocitrate FeMo-cofactor (FeMoCo) cluster (Fig. 1A). Importantly, FeMoCo operates as the Mo-N_2ase active site where substrates bind and undergo reduction. Fe protein is a homodimeric P-loop ATPase with a bridging [4Fe:4S] cluster and two nucleotide-binding sites sandwiched between the two subunits at the dimer interface. Fe protein is the obligate reductase for the N_2ase system, and ATP hydrolysis by the Fe protein is coupled to electron transfer to the MoFe protein metalloclusters ([4Fe:4S] cluster → P cluster → FeMoCo) and ultimately substrate reduction. Mo-N_2ase must undergo reduction of the FeMoCo active site for initial binding of substrates to the cofactor to occur. Notably, various substrates can be reduced by N_2ase, including N_2, C_2H_2, CN^-, N_3^-, and SCN^-. Unexpectedly, N_2ase can also catalyse C–C bond formation during the reduction of certain substrates, including CH_3NC and CO [17,18]; Einsle et al. have proposed a general mechanism for achieving C–C coupling [19]. Importantly, catalysis involves multiple sequential electron transfer steps that require the two-component proteins to form a transient complex, where electron transfer is coupled to ATP hydrolysis.

Work by Burris and coworkers on *Azotobacter vinelandii* purified Mo-N_2ase established that a central feature of the enzyme's kinetic mechanism involves dissociation of the Fe protein-MoFe protein complex [20]. They observed a lag phase in the production of H_2, and a quantitative assessment of the relationship between the length of the lag phase and duration of turnover led to the hypothesis that dissociation of the N_2ase protein complex is a necessary feature of biological nitrogen fixation. Their analysis of the electron paramagnetic resonance (EPR) signals from the active site of N_2ase during turnover indicated that each cycle of complex formation and dissociation is associated with electron transfer from the Fe protein to the MoFe protein active site [21] and that ATP hydrolysis is coupled to these electron transfer steps. To reset for the next cycle, the Fe protein FeS cluster must get reduced, typically by electron transfer from either a flavodoxin or ferredoxin, and MgADP must be exchanged with MgATP.

In the 1970s, Lowe and Thorneley utilized *Klebsiella pneumoniae* Mo-N_2ase to generate a thorough kinetic mechanism for N_2 reduction that is coupled with H_2 evolution [22]. This model was inspired by Joseph Chatt's framework for the reduction of N_2 proceeding through a sequence of electron–proton transfers in which N_2 binding is associated the with displacement of H_2 from the catalytic centre [23,24]. The Thorneley-Lowe model (summarized in Fig. 1B) postulates that

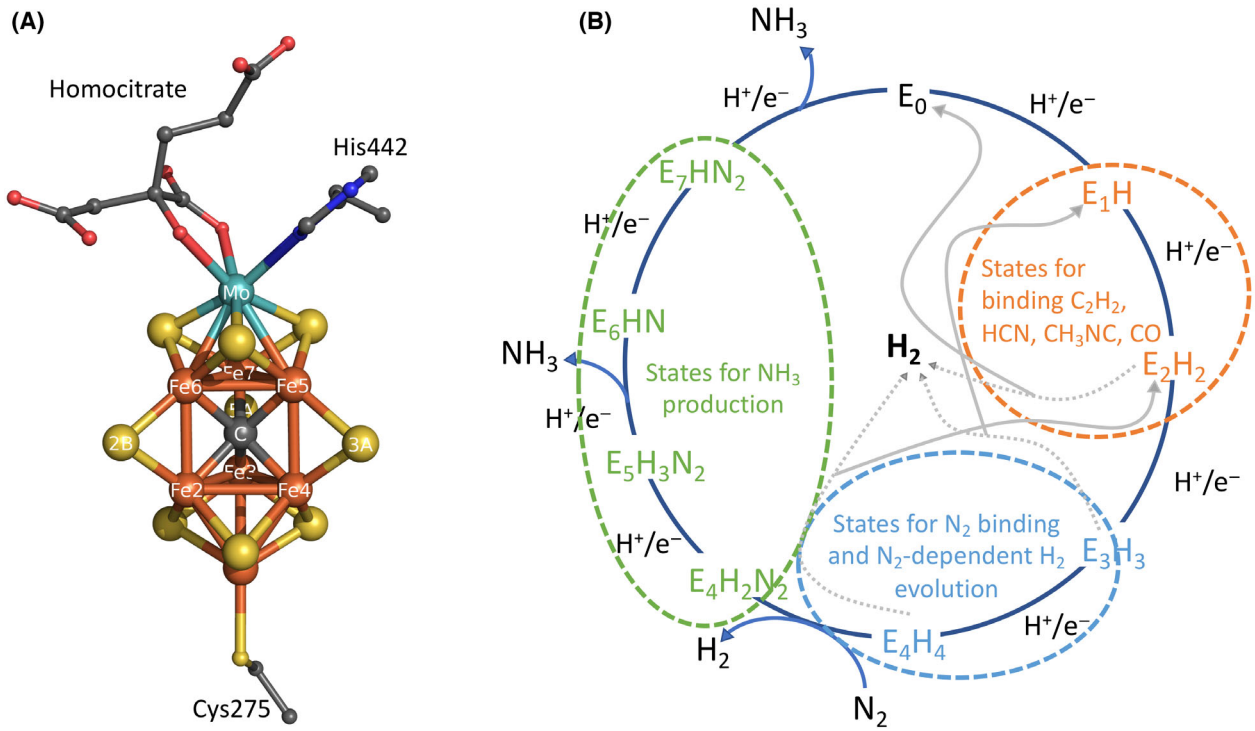

Fig. 1. FeMoCo active site structure and Thorneley-Lowe kinetic model for nitrogenase. (A) Structure of the FeMoCo active site and coordinating amino acids, Cys α275 and His α442, depicted in the E_0 ground state. Numbering of atoms and residues is based on PDB deposit 3U7Q, and sulfur is shown in yellow, iron in orange, carbon in grey, oxygen in red, nitrogen in blue and molybdenum in cyan. (B) Schematic representation of the Thorneley-Lowe model that describes the sequential eight-electron and hydrogen transfer processes (E_0–E_7) postulated to result in ammonia (NH_3) production catalysed by N_2ase. Importantly, reduction of the cluster to the E_3 or E_4 state is necessary for N_2 substrate binding to FeMoCo (circled in blue); however, other substrates have been found to bind the E_1 and E_2 states (circled in orange). H_2 evolution is hypothesized to occur in states E_2–E_4. H_2 evolution at the E_4 state occurs through a reductive elimination reaction accompanying the binding of N_2 to the metallocluster.

various reduced states of the MoFe protein (E_n) are generated throughout the N_2 fixation cycle, where n refers to the number of electron transfer steps from reduced Fe protein, relative to the as-isolated state (E_0) of the MoFe protein. It was proposed that eight electron transfer cycles are necessary for the production of two equivalents of NH_3 from N_2, coupled to the evolution of one H_2. Notably, N_2 does not bind to the as-isolated E_0 form of FeMoCo (the state that has been most extensively characterized crystallographically). Instead, three or four proton and electron transfers to the FeMoCo cluster (generating the E_3/E_4 states) were found to be required before nitrogen substrate binding can occur. Hydrogen evolution occurs from FeMoCo states E_2–E_4 and hence can take place in the absence of N_2 reduction. Other substrates, such as acetylene, cyanide, and isocyanides, have been found to bind to more oxidized forms of the MoFe-protein compared to states associated with either hydrogen evolution or N_2 binding [17,25,26].

Following the binding of N_2 through a reductive elimination reaction associated with H_2 evolution [27,28], a series of alternating proton and electron transfers would result in the production of two equivalents of NH_3. NH_3 is proposed to be released from some combination of E_5, E_6, and/or E_7 states. The rate-determining step for the sequential transition between E_n states ($k \sim 6.4\ s^{-1}$ at 23 °C for the *K. pneumoniae* system) was originally assigned as the dissociation of the Fe protein-MoFe protein complex [29], but it is now associated with phosphate dissociation from Fe protein [30]. By utilizing the physiological reductant flavodoxin protein in the hydroquinone state, Yang et al. were able to evaluate rate constants of each key step in the N_2ase reduction cycle and establish that phosphate dissociation from Fe protein after ATP hydrolysis is the rate limiting step. Additionally, this work indicated that the Fe protein only transfers a single electron to MoFe protein per ATP-hydrolysis cycle. Furthermore, the same Fe protein binding

interface was proposed to be used for MoFe protein and flavodoxin complexation [30].

Despite the ubiquity of the Thorneley-Lowe scheme in providing the kinetic framework for N_2ase, it is rarely used to quantitatively model experimental systems [16]. There are several reasons for this; most current experimental work employs *A. vinelandii* Mo-N_2ase assayed at 30 °C, while Thorneley and Lowe utilized the *K. pneumoniae* Mo-N_2ase at 23 °C. Independent attempts to quantitatively reproduce the reported kinetic fits were unsuccessful [31] and rapid freeze-quench EPR studies resulted in reassignment of what should have been the E_3 state based on kinetic modelling to the E_2 state [32,33]. Furthermore, FeMoCo states E_1 through E_7 were not directly detected and their existence was only inferred by Thorneley and Lowe; however, more recent spectroscopic experiments have observed E_1, E_2, E_4, E_7, and E_8 MoFe reduced states [9]. A modified version of the Thorneley-Lowe scheme has been developed by Hoffman and colleagues [9] that adds an E_8 state and only focuses on E_4 as competent for N_2 binding [33]. Additionally, a steady-state kinetic model for the *A. vinelandii* Mo-N_2ase has been recently described by Seefeldt and coworkers [14]. Taken together, these considerations indicate that the Thorneley-Lowe model should be treated as a working hypothesis that will continue to evolve as experimental knowledge is amassed.

Experimental insights are essential for framing hypotheses about the N_2ase reduction mechanism, and all current work postulates that the biological conversion of N_2 to NH_3 occurs through sequential N–H functionalization as opposed to initial N–N triple bond cleavage as seen within dissociative mechanisms, such as the Haber–Bosch process or through a multi-electron transfer step [34] (Fig. 2). Incremental weakening of the N–N bond through a sequence of coupled electron and proton transfers could proceed through distal, alternating, or hybrid reduction mechanisms [35,36]. The distal mechanism would involve one N of N_2 undergoing the first three hydrogenation steps to form and evolve NH_3, and the remaining nitrido-N is then hydrogenated three more times to produce the second NH_3. Conversely, the alternating pathway could involve alternating hydrogenations of N_2 where hydrogen transfers result in the stepwise formation of diazene (HNNH), hydrazine (H_2NNH_2), and then sequential production of NH_3. Finally, a potential hybrid mechanism could involve a combination of hydrogenation steps from the described distal and alternating mechanisms. The main cited evidence for partially reduced NN intermediates is based on acid and alkali quenching experiments of N_2ase under N_2 turnover conditions yielding hydrazine [8,37]; however, this is not a conclusive demonstration that hydrazine is an on-path N_2ase intermediate, as hydrazine is known to be generated during acid quenching studies of well-characterized, synthetic N_2 binding complexes [38].

Biochemical and spectroscopic studies continue to focus on evaluating the properties of various N_2ase intermediates that are proposed to form during the Mo-N_2ase reduction mechanism. In particular, the "2N2H" intermediate has been assigned to the E_4 state and proposed to correspond to a dinitrogen dihydride

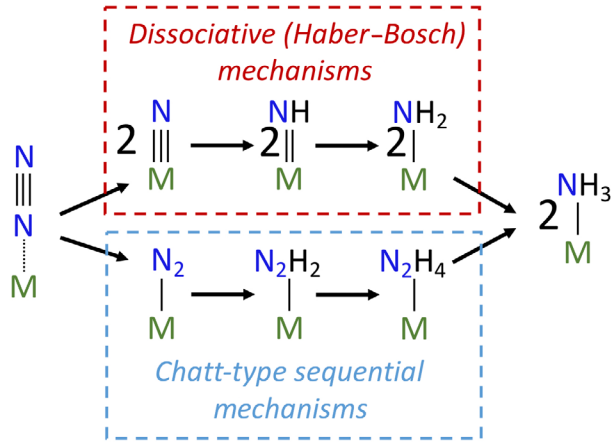

Fig. 2. Possible mechanisms for N_2 reduction to NH_3. (Top) Dissociative mechanism typically associated with the Haber–Bosch process in which the N–N triple bond is cleaved during an initial step of the mechanism. (Bottom) Chatt-type sequential mechanisms can proceed through distal, alternating, and hybrid pathways in which the N–N triple bond is progressively weakened *via* sequential hydrogenation (depicted using addition of pairs of H for simplicity). Variations include an initial reduction by multiple electrons, but without complete cleavage of the N–N triple bond [34], or reduction of N_2 by a reaction other than hydrogenation [118].

or diazene-level intermediate [39]. Furthermore, a second E_4 state that contains two hydrides, but no bound N substrate, has been characterized using freeze-quenched EPR studies; this resulted in a hypothesis that reductive elimination of H_2 is necessary for the generation of sufficiently reduced Fe centres for N_2 binding, ultimately resulting in an E_4 (2N2H) species. Importantly, E_5 and E_6 level intermediates that represent the subsequent steps in the reduction mechanism have yet to be detected.

X-ray crystallographic studies have provided detailed structures of the N_2ase component proteins, including the constituent metallocofactors, as well as more recent crystal structures of ligand-bound forms of N_2ase enzymes that have provided crucial mechanistic insights [10]. The first ligand-bound Mo-N_2ase structure revealed that carbon monoxide (CO), a known inhibitor of N_2ase substrates, becomes ligated between Fe2 and Fe6 atoms of FeMoCo in a μ_2-fashion replacing the S2B belt sulfur and resulting in hydrogen bonding between the O atom of the CO ligand and the imidazole of His195 [40]. Significantly, this region was implicated in substrate binding by Dean and colleagues based on the isolation and characterization of acetylene-resistant mutants [41]. This work further builds upon infrared (IR), EPR, and electron-nuclear double resonance (ENDOR) studies of Mo-N_2ase that had previously reported evidence of CO binding to a FeMoCo metal centre when subjected to various pressures of CO under turnover conditions [42–49]. It is important to recognize, however, that crystallographic characterization of this species required a time scale of hours, which is much longer than the onset of inhibition (< 100 ms) and the time associated with appearance of the characteristic EPR signals of the CO inhibited state (~ 4 s) [42]. Interestingly, spectroscopic studies of CO-inhibited MoFe protein in which the interstitial carbide is ^{13}C enriched revealed that the process for CO incorporation at the belt sulfur positions does not involve major rearrangements of the CFe_6 core [50]. Subsequent studies have confirmed the importance of the S2B site in ligand binding in both Mo-N_2ase [51] and V-N_2ase systems [19,52,53]. In particular, V-N_2ase studies have shown FeVCo is able to bind CO at the 2B position in the resting state. Interestingly, FeVCo does not require cluster reduction before ligand binding as observed with FeMoCo, likely due to a lower average valency of the Fe centres in FeVCo ($V^{3+}3Fe^{3+}4Fe^{2+}$) compared to FeMoCo ($Mo^{3+}4Fe^{3+}3Fe^{2+}$) [54,55]. Taken together, these experiments highlight the privileged role in the binding of exogenous ligands played by Fe2 and Fe6 in the trigonal prism of the FeMoCo.

Additional structural studies with selenocyanate ($SeCN^-$) have unambiguously demonstrated that exogenous ligands can become incorporated into the belt positions, especially S2B. In particular, when N_2ase is incubated with $SeCN^-$ under turnover conditions, Se is initially incorporated primarily, but not exclusively, at the S2B position. When the Se2B-labeled MoFe protein is subsequently subjected to turnover in the presence of acetylene, Se migration to the S5A and S3A belt sulfur positions is observed [56]. Alternatively, when the Se2B-labeled protein and active site are treated with CO, Se migrates to the S5A and S3A positions as opposed to being removed from the cofactor; this result suggests a process in which the cofactor either rearranges to exchange the belt positions or an overall rotation of the cofactor within the active site takes place. While the exact mechanism for FeMoCo belt sulfur rearrangements remains enigmatic, these $SeCN^-$ and CO N_2ase ligand studies generally establish that Fe–S bonds are labile and structural rearrangements can occur within the FeMoCo active site during turnover [56,57]. Further work is needed, however, to establish whether the belt sulfur displacement observed in these ligand binding studies represents an "on-path" state in the N_2 reduction mechanism or is representative of "off-path" species formed under these experimental conditions.

Limitations of N_2ase experimental studies

While experimental studies of N_2ase have undoubtedly provided crucial insights, it is important to recognize that many details of the reduction mechanism remain elusive. Indeed, the combination of the small size of the dinitrogen substrate, the inability of the as-isolated form of FeMoCo to bind N_2, and the impressive complexity of the active site have hindered the deciphering of an atomic-level understanding of the biological mechanism for N_2 reduction. Furthermore, at steady state, a mixture of states (E_0–E_7) will be present, making concrete interpretations of biochemical and spectroscopic data very challenging. The presence of the P-cluster ([8Fe:7S]) and 4Fe4S clusters of the Fe protein further complicate the analysis of spectroscopic data, as does the prediction that approximately half of the Mo-N_2ase N_2 substrate intermediates will be even-electron and thus "dark" when analysed with spin resonance techniques. Signal relaxation-broadening above 25 K further confounds spectroscopic analysis of vital Fe–N species [58]. Notably, studies of dithionite-reduced FeFeCo revealed that Fe-N_2ase has an integer spin ground state likely caused by antiferromagnetic

coupling between the cofactor Fe atoms that results in odd-electron states (E_1, E_3, E_5, E_7) rather than even-electron states (E_0, E_2, E_4, E_6) being paramagnetic and spin-resonance technique active [59]. Resultingly, spin resonance studies that couple data from the MoFe and FeFe proteins should allow for all relevant reduced states of the N_2ase cofactor to be fully characterized. Additionally, it has been well-documented that the nitrogenase proteins exhibit considerable oxygen sensitivity and thus must be manipulated within anaerobic environments. Most N_2ase protein samples are accordingly supplemented with dithionite ($Na_2S_2O_4$) in order to prevent O_2 contamination [60,61]. Dithionite (DT) is known to gradually decompose within aqueous solutions to a variety of S-containing species, including sulphite (SO_3^{2-}), sulfate (SO_4^{2-}), and sulphide (S^{2-}) [60,62], and these decomposition products have the potential to react with the FeMoCo under turnover conditions, which could prevent detection and isolation of activated, reduced forms of the cofactor.

Together, experimental studies of Mo-N_2ase indicate that a complex sequence of proton and electron transfer steps associated with hydride formation, and likely coupled with cofactor rearrangement, govern activation of N_2; however, few details are known about the intermediate FeMoCo turnover states. Given the small sizes of N_2ase substrates and the existence of multiple conformational states under turnover conditions, approaches are limited for detailed experimental characterization of substrate reduction intermediates. Thus, computational techniques serve a crucial role in elucidating the specific mechanistic steps of biological nitrogen fixation. Importantly, theoretical studies have previously clarified mechanistic steps of redox-active enzymes involving multiple electron and proton transfer steps, such as photosystem II [63–65]. Given the limitations of current experiments to provide detailed characterization of FeMoCo reduction intermediates, their integration with complementary computational studies is essential to further illuminate the complicated process of N_2ase reduction.

Computational insights into nitrogenase reduction of N_2

As we have discussed, experimental investigations of N_2ase serve as the basis for framing the chemical mechanism of biological nitrogen fixation. Despite substantial experimental efforts towards elucidating specific details of this system, including N_2 binding to the cofactor concomitant with release of H_2, N–N bond cleavage and N–H bond formation *via* iterative proton and electron transfer steps, and release and transport of NH_3 to the protein surface, many features of the N_2 fixation mechanism require further validation. As such, computational studies of the N_2ase system are essential for simulating proposed reactions and pathways to illuminate the atomic details of the molecular mechanism of biological nitrogen fixation.

The accumulation of protons and electrons on FeMoCo is key to priming the active site for substrate binding and results in the formation of a variety of E_nH_n species. One key advantage of computational studies is the ability to simulate and evaluate a single, pure intermediate species and thereby assess its mechanistic feasibility and relevance. Various quantum mechanics (QM) and quantum mechanics/molecular mechanics (QM/MM) model studies have explored these E_nH_n structures to determine the likely sites for proton and hydride accumulation prior to N_2 binding. Ryde and Cao have established that the resting state (E_0) is deprotonated and the E_1H_1 state has one H on belt sulfur S2B, which affords > ~ 20 kJ·mol^{-1} energy stabilization [66]. Studies of substrate-free E_2H_2, E_3H_3, and E_4H_4 states in particular have revealed the importance of functional choice in density functional (DF) calculations of FeMoCo. The pure TPPS functional often favours structures with Fe–H bonds, whereas hybrid functionals like B3LYP tend to significantly favour formation of C–H bonds by the interstitial carbon [66]. Ultimately, given the large number of possible combinations of geometrical and electronic structures of FeMoCo, a conclusive understanding of the electronic and structural states that correspond to E_1H_1 through E_4H_4 have yet to be determined; however, some consistent trends are evident in the computational findings. For instance, formation of S2B-H is energetically favourable, when S3B is protonated it consistently loses a bond to Fe not Mo, and calculations where the electronic state is defined initially often undergo changes during optimization to a different electronic state or related geometrical structure [67].

An essential step of each N_2 reduction cycle involves an N_2 molecule navigating from the protein surface to the FeMoCo active site. Computational simulations and examination of the crystallographic binding sites of small molecules, such as xenon, to the MoFe-protein have revealed multiple potential substrate channels, including a hydrophobic path that leads to the Fe2 position of FeMoCo [68–74]. Free energy analyses of N_2 moving from the protein surface to FeMoCo through this channel have revealed extremely low activation-free energy barriers (~ 12 kJ·mol^{-1}), further supporting feasibility of this path as an N_2 ingress channel [68,70]. Fe2 has been implicated as an important site for N_2 binding based on multiple

computational studies; details of the potential roles of Fe2 in the N_2ase mechanism are discussed in greater detail in the full mechanism section below [75]. Relatedly, DF studies focused on the role of the interstitial carbide (C^c) have revealed hydrogenation, and the binding of substrates and intermediates results in coordinative allosterism within FeMoCo. For example, DF studies have shown that N_2 binding to Fe2 results in weakening and elongation of the Fe2–C^c bond and compensatory strengthening and shortening of the Fe6–C^c bond; satisfying a proposed five bond optimum bonding capacity of the C^c to Fe atoms in FeMoCo [67,76]. Note that studies where the interstitial carbide of FeMoCo is ^{13}C labelled indicate the CFe_6 cluster core does not experience significant rearrangements within the states that have been examined spectroscopically [50].

The physiological process of N_2 reduction requires eight proton transfer steps to produce $2NH_3$ and $1H_2$. DF calculations have explored mechanisms for serial supply of protons to FeMoCo, and His195, the closest side chain to the FeMoCo cluster, is anticipated to have a pK_a in the physiological range, that would likely allow for at least one proton transfer step [77,78]. It has been postulated that the relative high acidity of the protonated imidazole may indicate hydrogen transfer from His195 represents the first and most difficult reduction step in the N_2 fixation process (NNH formation); however, simulations have hypothesized that continual relay of protons from His195 may require a complete imidazole flip, which has a higher energy barrier [78]. Consequently, other proton supply mechanisms have been explored, and a water chain that connects the protein surface to S3B has been identified and analysed. This single chain of eight hydrogen-bonding water molecules has been strictly conserved across all reported crystal structures of MoFe protein [79]. It is proposed that this water chain acts as a proton wire that allows for hydrogens to accumulate on S3B *via* the standard Grotthuss mechanism [80,81]. A 269-atom DF model that included all pertinent residues near the water chain revealed that there were low potential energy barriers (< 30 kJ·mol^{-1}) for proton movement across the wire; this process also included the participation of carboxylate groups of the homocitrate. Notably, once S3B-H is formed, the H atom can move to different sites on S3B, which allows for hydrogen transfer to other sites within FeMoCo. DF studies of the various S3B-H configurations revealed that the potential energy surface barriers for H bond movement are small, and one key simulated H atom transfer pathway involved hydrogen movement from S3B to Fe6 and finally to S2B and Fe2, which could allow for hydrogenation of substrates and intermediates [80,82,83]. Ultimately, computational studies of hydrogen accumulation processes for FeMoCo have clarified our understanding of potential roles for His195, *R*-homocitrate, and the conserved water chain adjacent to FeMoCo as crucial towards the formation of $E_nH_nN_x$ intermediates.

Finally, computational studies have explored the NH_3 exit pathway and identified a homocitrate-associated pool of water molecules that are believed to assist in the egress of the ammonia product [74]. Analysis of the protein tertiary structure and probable dynamic fluctuations associated with NH_3 transport to the protein surface have been modelled. The relatively high B factors of this region support conformational flexibility potentially associated with the N_2ase mechanism and NH_3 product egress. Insights regarding the FeMo-cofactor structure and roles of various components of the active site are summarized in Fig. 3 (adapted from [83]).

Comparing computationally proposed N_2 reduction mechanisms

Dance [79] has reviewed a collection of computationally-based N_2 reduction mechanism proposals, including work by Blöchl, Kästner et al. [84–87], Nørskov et al. [88,89]. and Adamo et al. [90]. Here, we will discuss selected features of these mechanisms, including recently published updates. Work by Dance investigating the association between N_2 binding and Fe–S bond lability revealed the importance of multi-atom rearrangements. The DF calculations were based on experimentally derived structural features, including a core cluster ($[Fe_7MoS_9C]$) charge of -1, net E_0 spin state of $S = 3/2$, atomic coordinates from the 1 Å resolution 3U7Q PDB X-ray crystal structure (486-atoms total), and mutagenesis and structural studies that implicate the Fe2-Fe3-Fe6-Fe7 face as the catalytic reaction zone of FeMoCo [32,91–94]. Given that Fe2 is located near a probable channel for ingress diffusion of N_2 and His195 can provide hydrogen bonding to a Fe2-coordinated substrate, N_2 binding to the Fe2 position was simulated. Initially, FeMoCo was modelled to have a hydrogen bridging Fe2 and Fe6 and an additional hydrogen binding to S2B, the belt sulfur that connects Fe2 and Fe6. Upon equilibration of N_2 within the ingress channel (initial distance 3 Å), N_2 was found to bind Fe2 end-on with a very small energy barrier (12 kJ·mol^{-1} when $S = 1/2$ or 16 kJ·mol^{-1} $S = 3/2$), accompanied by dissociation of S2B-H from Fe2 [75]. Notably, more extensive rearrangements that would lead to internal scrambling of the belt positions were found to have a high barrier and

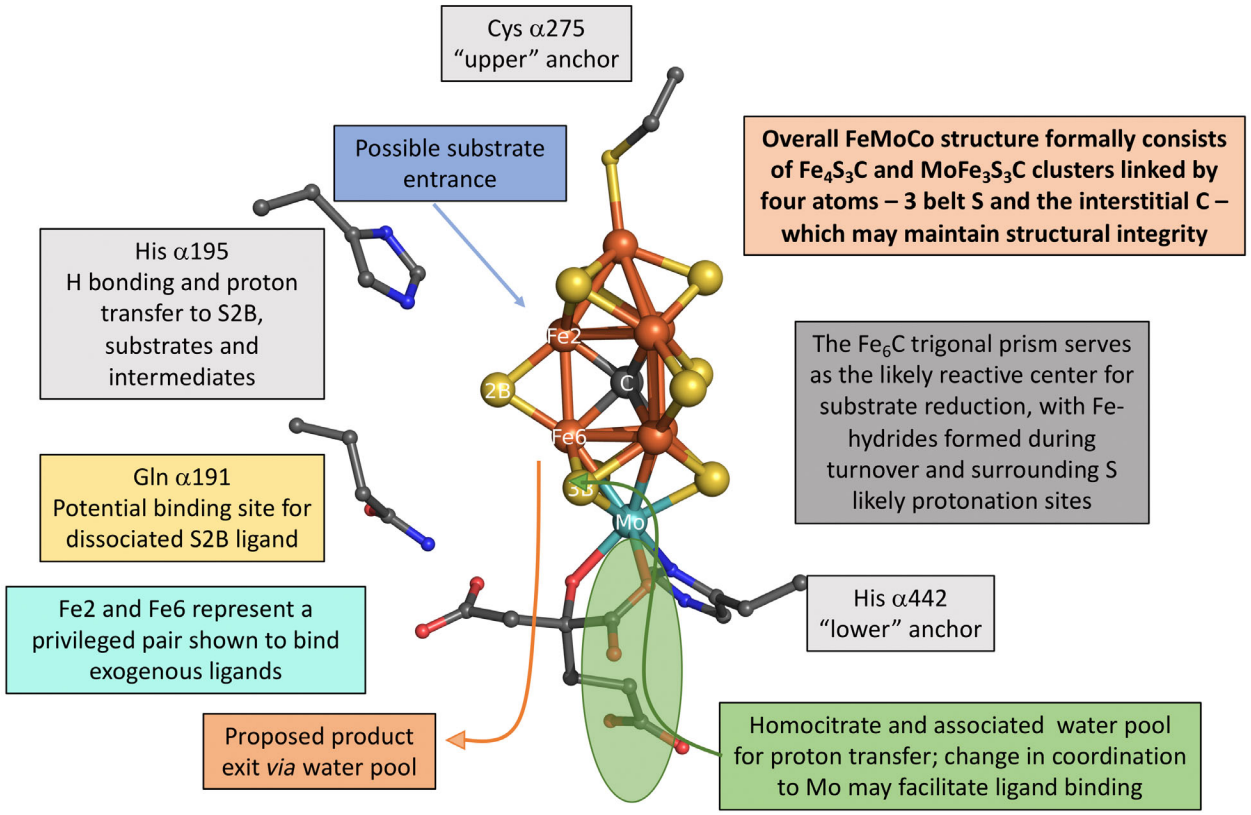

Fig. 3. Summary of the mechanistic roles of structural components within the nitrogenase active site. Proposed mechanistic functions and roles for key features of the FeMoCo active site, including His α195, Gln α191, Cys α275, His α442, FeMoCo water pools, homocitrate, interstitial carbide, as well as the overall cofactor structure are outlined. Figure adapted from Dance 2020 review [79].

hence would be unlikely to occur [95]. More recent work by Dance has explored the possibility that the N_2 molecule that initially binds Fe2 *via* the substrate channel may not be reduced, but instead could play a promotional role in expanding the reaction zone [96]. This mechanism proposes that a second N_2 enters *via* the ingress channel and binds to Fe6, where it is primed for intramolecular hydrogen transfer from atoms originating on S3B, culminating in reduction from N_2 to NH_3 [96].

A critical feature in the N_2ase mechanism of Siegbahn concerns the role of the interstitial carbide. By analysing models with 160–270 atoms using the B3LYP hybrid functional, Siegbahn has identified a mechanism in which C^c becomes hydrogenated to a methyl group that shifts to the periphery of the cluster core while bound to Fe6 (*exo*-Fe6) [77,97,98]. Subsequently, N_2 substrate binding and hydrogenation are proposed to proceed within the now empty central region. Importantly, formation of CH_3 is categorized as an "activation phase" that is equivalent to the E_0 state. The mechanism then proceeds *via* hydrogenation steps that mimic the Thorneley-Lowe model, and E_4-H_2/E_4-N_2 exchange is included. The distinctive structural features of this Siegbahn hydrogenation cycle include the role of CH_3 bound *exo* to Fe6, unhooking of S2B-H from Fe6 during the hydrogenation and rehooking afterwards, as well as generation of five-coordinate Mo due to partial dissociation of the homocitrate alcohol group [79]. Wei and Siegbahn recently reported an additional analysis of the initial four reduction activation steps (generating E_0) that resulted in loss of a sulfide (H_2S3A) as opposed to protonation of C^c to a methyl group. This builds upon experimental studies that showed the inhibitor CO can replace S2B [40]. Simulation of N_2 binding revealed that the nitrogen substrate binds too weakly to force loss of a sulfide; however, CO binds significantly more strongly to FeMoCo and successfully displaces the sulfide in an almost thermoneutral step based on these DF studies. Overall, the four activation steps were found to result in a very weakly bound sulfide that could be released in a significantly exergonic step (−-50 $kJ{\cdot}mol^{-1}$). This study found that the barrier for protonation of the carbide beyond CH was much

higher than sulfur protonation. Additionally, after sulfide loss, the catalysis cycle was modelled to commence *via* N_2 binding to Fe4, one of the most reduced Fe atoms in this system. Notably, sulfide loss was also associated with hydrides preferring a bridging position, which had a stabilizing effect on the overall cluster [99]. It should be noted that an *exo* Fe-CH_3 group would likely be hydrolytically unstable and a detailed mechanism for regeneration of the E_0 resting state has yet to be clearly outlined [79].

Ryde has explored the N_2ase reduction mechanism using computational studies, with recent work focusing on the potential role of the μ_2-bridging S2B position in substrate binding and reduction [100–102]. In particular, a QM/MM approach (133 915 atoms) was paired with QM calculations (170–178 atoms), where two DF methods were employed: the non-empirical, pure functional TPSS and the hybrid B3LYP functional, to explore the optimized energies and geometries of a wide range of NNX-bound E_4 structures. This full N_2ase mechanism is proposed to begin with N_2 binding in a "half-bridging" mode within the empty S2B site. N_2H_2 is then produced using intramolecular hydrogen transfer from protons already present on the cluster with the first protonation requiring approximately 17 $kJ{\cdot}mol^{-1}$ of energy. Interestingly, Cao and Ryde suggest N_2 hydrogenation most favourably proceeds from intermediate NNH_2 bound end-on to H_2NNH in a side-on bridging conformation (Fe2/Fe6). Formation of H_2NNH_2 (hydrazine) was then reported to be the most stable subsequent structure, and the next reduction step facilitated facile cleavage of the NN bond resulting in NH_3 bound solely to Fe2 and NH_2^- stabilized by a bridging conformation between Fe2 and Fe6. The final mechanistic step involves NH_3 dissociation and protonation of NH_2^- to NH_3, but only after S2B rebinds to the cluster. Overall, this work proposed a hybrid mechanism, in which E_5-E_7 states favour an alternating mechanism (with the exception of NNH_2 being reported as the most stable N_2H_2 state), while other steps in the mechanism suggest a distal approach, such as favourable formation of NNH_3. This computational work builds upon experimental studies to suggest N_2 could bind to an empty S2B site and coordination of nitrogen substrate between Fe2 and Fe6 atoms may facilitate the formation of two NH_3 molecules *via* an energetically favourable mechanism.

Limitations of N_2ase computational studies

Computational studies avoid many of the limitations inherent with experiments and can provide novel insights into the unprecedented structure and coordination chemistry of FeMoCo. As detailed above, various theoretical analyses of the N_2ase system have provided important insights ranging from identification of likely substrate ingress and egress channels to proposed detailed mechanisms for the entire reduction process; however, computational analyses are also not without limitations. Each of these studies involves constraining the parameters of the nitrogenase system based upon the focus of that particular study, such as deciding the number of atoms used (model size), choice of functional and basis set, defining the overall model charge, and choice of solvation dielectric constant. Defining the functional choice, particularly hybrid vs. pure, has been found to especially influence which FeMoCo structures and bonds are energetically and geometrically favoured with wide variations reported (> 200 $kJ{\cdot}mol^{-1}$) [103]. As such, this review has focused on key features of mechanisms that have been proposed through computational studies. Clearly, these features cannot all be correct, but they highlight aspects of the mechanism that can ultimately be validated through an iterative process of hypothesis revision coupled with continued advances in both computational and experimental studies.

Outstanding questions and future studies

Advances in experimental and computational techniques have aided our understanding of several facets of biological nitrogen fixation. Given the complexity of the metallocluster active site and current inability to trap mechanistically relevant intermediates, outstanding questions regarding the N_2ase system include:

1 What are the mechanistically relevant intermediates for N_2 fixation? Current models have singularly focused on a general mechanism where N_2 reduction proceeds through a sequence of proton and electron transfers, but it must be noted that no definitive evidence for any on-path, partially reduced NN intermediate has been presented.
2 Does the cofactor rearrange during turnover? In particular, how do the belt sulfurs exchange/interchange during turnover? Does the CFe_6 core remain rigid throughout N_2 reduction?
3 Does each cycle of reduction by the Fe protein result in the coupled transfer of one proton and one electron to the FeMoCo, as typically modeled?
4 What is the exact role of His195 within the substrate reduction mechanism? Can this residue supply multiple hydrogens to the cofactor?

5 Is the H_2/N_2 exchange step accompanied by hydrogenation of N_2? Is this a unique reaction associated with N_2 reduction, or do other substrates also display this property?
6 What are the roles of homocitrate in the substrate reduction mechanism?

These queries represent only a few of the unresolved details regarding this system, and future experiments will need to combine findings from Mo-N_2ase experimental and computational work, as well as evaluations of the Fe-N_2ase and V-N_2ase systems, in order to advance our knowledge of this process. There are a number of promising approaches to further illuminate steps in the N_2ase mechanism. Experimentally, strategies for the site-specific labelling of various atoms in the FeMo-cofactor, including iron [104], molybdenum [105], carbon [50,106], sulfurs (including selenium incorporation) [56,57,62], and homocitrate [107] will allow for transformative spectroscopic and structural studies that should yield insights into bonding interactions, rearrangements, and potentially allow for substrate coordination sites to be monitored. Another arena for important experimental advances is in the development of Fe protein-independent systems that utilize a photo-activated supply of electrons [108,109] or electrocatalysis [110,111] to reduce the MoFe protein; this would allow for the electron supply to be better controlled to more effectively generate homogenous samples in defined E_n states for analysis. The recent revolution in electron microscopy is opening up structural studies of solutions of nitrogenase in defined states [112–114], as well as under turnover conditions [114]. Computational analyses will benefit from advances that allow for more realistic treatment of complex metalloclusters [115,116], as well as to incorporate more of the surrounding protein and account for the dynamics of the protein structure on the chemistry within the active site. Computational and experimental studies will both benefit from synthetic FeS clusters that mimic FeMoCo and support the binding [117] and particularly the reduction of N_2 [118]. Ultimately, the integration of experimental and computational studies will be essential for the identification and analysis of relevant intermediate species that are central to the N_2ase mechanism for biological nitrogen fixation.

Acknowledgments

We thank Dr Rebecca Warmack, Dr Trixia Buscagan, Dr Siobhan MacArdle and Ailiena Maggiolo for discussions, and Prof William Goddard and Charles Musgrave for their invaluable advice and insights on density functional calculations on nitrogenase. This work was supported by the Howard Hughes Medical Institute.

References

1 Holland PL. Introduction: reactivity of nitrogen from the ground to the atmosphere. *Chem Rev*. 2020;**120**:4919–20.
2 Zhang X, Ward BB, Sigman DM. Global nitrogen cycle: critical enzymes, organisms, and processes for nitrogen budgets and dynamics. *Chem Rev*. 2020;**120**:5308–51.
3 Kalescky R, Kraka E, Cremer D. Identification of the strongest bonds in chemistry. *J Phys Chem A*. 2013;**117**:8981–95.
4 Capdevila-Cortada M. Electrifying the Haber–Bosch. *Nat Catal*. 2019;**2**:1055.
5 Boerner LK. Industrial ammonia production emits more CO_2 than any other chemical-making reaction. Chemists want to change that. *Chem Eng News*. 2019;**97**:1–7.
6 Jennings JR. Catalytic ammonia synthesis. New York: Springer; 1991.
7 Studt F, Tuczek F. Energetics and mechanism of a room-temperature catalytic process for ammonia synthesis (schrock cycle): comparison with biological nitrogen fixation. *Angew Chem Int Ed Engl*. 2005;**44**:5639–42.
8 Burgess BK, Lowe DJ. Mechanism of molybdenum nitrogenase. *Chem Rev*. 1996;**96**:2983–3011.
9 Seefeldt LC, Yang ZY, Lukoyanov DA, Harris DF, Dean DR, Raugei S, et al. Reduction of substrates by nitrogenases. *Chem Rev*. 2020;**120**:5082–106.
10 Einsle O, Rees DC. Structural enzymology of nitrogenase enzymes. *Chem Rev*. 2020;**120**:4969–5004.
11 Jasniewski AJ, Lee CC, Ribbe MW, Ribbe MW, Hu Y. Reactivity, mechanism, and assembly of the alternative nitrogenases. *Chem Rev*. 2020;**120**:5107–57.
12 Van Stappen C, Decamps L, Cutsail GE, Bjornsson R, Henthorn JT, Birrell JA, et al. The spectroscopy of nitrogenases. *Chem Rev*. 2020;**120**:5005–81.
13 Burén S, Jiménez-Vicente E, Echavarri-Erasun C, Rubio LM. Biosynthesis of nitrogenase cofactors. *Chem Rev*. 2020;**120**:4921–68.
14 Harris DF, Badalyan A, Seefeldt LC. Mechanistic insights into nitrogenase FeMo-cofactor catalysis through a steady-state kinetic model. *Biochemistry*. 2022;**61**:2131–7.
15 Harris DF, Lukoyanov DA, Kallas H, Trncik C, Yang Z, Compton P, et al. Mo-, V-, and Fe-nitrogenases use a universal eight-electron reductive-elimination mechanism to achieve N_2 reduction. *Biochemistry*. 2019;**58**:3293–301.

16 Buscagan TM, Rees DC. Rethinking the nitrogenase mechanism: activating the active site. *Joule*. 2019;**3**:2662–78.
17 Rubinson JF, Corbin JL, Burgess BK. Nitrogenase reactivity: methyl isocyanide as substrate and inhibitor. *Biochemistry*. 1983;**22**:6260–8.
18 Hu Y, Lee CC, Ribbe MW. Extending the carbon chain: hydrocarbon formation catalyzed by vanadium/molybdenum nitrogenases. *Science*. 2011;**333**:753–5.
19 Rohde M, Laun K, Zebger I, Stripp ST, Einsle O. Two ligand-binding sites in CO-reducing V nitrogenase reveal a general mechanistic principle. *Sci Adv*. 2021;**7**: eabg4474.
20 Hageman RV, Burris RH. Nitrogenase and nitrogenase reductase associate and dissociate with each catalytic cycle. *Proc Natl Acad Sci USA*. 1978;**75**:2699–702.
21 Hageman RV, Burris RH. Changes in the EPR signal of dinitrogenase from *Azotobacter vinelandii* during lag period before hydrogen evolution begins. *J Biol Chem*. 1979;**254**:11189–92.
22 Thorneley RNF, Lowe DJ. Kinetics and mechanisms of the nitrogenase enzyme system. In: Spiro T, editor. Molybdenum enzymes. New York: John Wiley & Sons, Inc; 1985. p. 221–84.
23 Chatt J, Dilworth JR, Richards RL. Recent advances in the chemistry of nitrogen fixation. *Chem Rev*. 1978;**78**:589–625.
24 Chatt J. Nitrogen fixation. In: Stewart WDP, Gallon JR, editors. Proceedings of the phytochemical society of Europe symposium, September, 1979. London: Academic Press; 1980.
25 Lowe DJ, Fisher K, Thorneley RNF, Vaughn SA, Burgess BK. Kinetics and mechanism of the reaction of cyanide with molybdenum nitrogenase from *Azotobacter vinelandii*. *Biochemistry*. 1989;**28**:8460–6.
26 Lowe DJ, Fisher K, Thorneley RNF. *Klebsiella pneumoniae* nitrogenase. Mechanism of acetylene reduction and its inhibition by carbon monoxide. *Biochem J*. 1990;**272**:621–5.
27 Harris DF, Yang ZY, Dean DR, Seefeldt LC, Hoffman BM. Kinetic understanding of N_2 reduction versus H_2 evolution at the E4(4H) Janus state in the three nitrogenases. *Biochemistry*. 2018;**57**:5706–14.
28 Lukoyanov D, Khadka N, Yang ZY, Dean DR, Seefeldt LC, Hoffman BM. Reductive elimination of H_2 activates nitrogenase to reduce the N≡N triple bond: characterization of the E4(4H) Janus intermediate in wild-type enzyme. *J Am Chem Soc*. 2016;**138**:10674–83.
29 Thorneley RN, Lowe DJ. The mechanism of *Klebsiella pneumoniae* nitrogenase action. Pre-steady-state kinetics of an enzyme-bound intermediate in N_2 reduction and of NH_3 formation. *Biochem J*. 1984;**224**:887–94.
30 Yang ZY, Ledbetter R, Shaw S, Pence N, Tokmina-Lukaszewska M, Eilers B, et al. Evidence that the pi release event is the rate-limiting step in the nitrogenase catalytic cycle. *Biochemistry*. 2016;**55**:3625–35.
31 Wilson PE, Nyborg AC, Watt GD. Duplication and extension of the Thorneley and Lowe kinetic model for *Klebsiella pneumoniae* nitrogenase catalysis using a MATHEMATICA software platform. *Biophys Chem*. 2001;**91**:281–304.
32 Fisher K, Newton WE, Lowe DJ. Electron paramagnetic resonance analysis of different *Azotobacter vinelandii* nitrogenase MoFe-protein conformations generated during enzyme turnover: evidence for S = 3/2 spin states from reduced MoFe-protein intermediates. *Biochemistry*. 2001;**40**:3333–9.
33 Hoffman BM, Lukoyanov D, Yang ZY, Dean DR, Seefeldt LC. Mechanism of nitrogen fixation by nitrogenase: the next stage. *Chem Rev*. 2014;**114**:4041–62.
34 Shilov AE. Catalytic reduction of molecular nitrogen in solutions. *Russ Chem Bull*. 2003;**52**:2555–62.
35 Jia HP, Quadrelli EA. Mechanistic aspects of dinitrogen cleavage and hydrogenation to produce ammonia in catalysis and organometallic chemistry: relevance of metal hydride bonds and dihydrogen. *Chem Soc Rev*. 2014;**43**:547–64.
36 Van Der Ham CJM, Koper MTM, Hetterscheid DGH. Challenges in reduction of dinitrogen by proton and electron transfer. *Chem Soc Rev*. 2014;**43**:5183–91.
37 Thorneley RNF, Eady RR, Lowe DJ. Biological nitrogen fixation by way of an enzyme-bound dinitrogen-hydride intermediate. *Nature*. 1978;**272**:557–8.
38 Deneke CF, Krinsky NI. Reduction of molecular nitrogen to hydrazine. Structure of a dinitrogen complex of bis(pentamethylcyclopentadienyl)zirconium (II) and an ^{15}N labeling study of its reaction with hydrogen chloride. *J Am Chem Soc*. 1976;**98**:3042–4.
39 Lukoyanov D, Yang ZY, Khadka N, Dean DR, Seefeldt LC, Hoffman BM. Identification of a key catalytic intermediate demonstrates that nitrogenase is activated by the reversible exchange of N_2 for H_2. *J Am Chem Soc*. 2015;**137**:3610–5.
40 Spatzal T, Perez KA, Einsle O, Howard JB, Rees DC. Ligand binding to the FeMo-cofactor: structures of CO-bound and reactivated nitrogenase. *Science*. 2014;**345**:1620–3.
41 Christiansen J, Cash VL, Seefeldt LC, Dean DR. Isolation and characterization of an acetylene-resistant nitrogenase. *J Biol Chem*. 2000;**275**:11459–64.
42 Davis LC, Davis LC, Henzl MT, Burris RH, Orme-Johnson WH. Iron-sulfur clusters in the

molybdenum-iron protein component of nitrogenase. Electron paramagnetic resonance of the carbon monoxide inhibited state. *Biochemistry*. 1979;**18**:4860–9.
43 Pollock RC, Orme-Johnson WH, Lee HI, DeRose VJ, Hoffman BM, Cameron LM, et al. Investigation of CO bound to inhibited forms of nitrogenase MoFe protein by ^{13}C ENDOR. *J Am Chem Soc*. 1995;**117**:8686–7.
44 George SJ, Ashby GA, Wharton CW, Thorneley RNF. Time-resolved binding of carbon monoxide to nitrogenase monitored by stopped-flow infrared spectroscopy. *J Am Chem Soc*. 1997;**119**:6450–1.
45 Yan L, Dapper CH, George SJ, Wang H, Mitra D, Dong W, et al. Photolysis of Hi-CO nitrogenase – observation of a plethora of distinct CO species using infrared spectroscopy. *Eur J Inorg Chem*. 2011;**2011**:2064–74.
46 Yan L, Pelmenschikov V, Dapper CH, Scott AD, Newton WE, Cramer SP. IR-monitored photolysis of CO-inhibited nitrogenase: a major EPR-silent species with coupled terminal CO ligands. *Chemistry*. 2012;**18**:16349–57.
47 Christie PD, Lee HI, Cameron LM, Hales BJ, Orme-Johnson WH, Hoffman BM. Identification of the CO-binding cluster in nitrogenase MoFe protein by ENDOR of ^{57}Fe isotopomers. *J Am Chem Soc*. 1996;**118**:8707–9.
48 Lee HI, Cameron LM, Hales BJ, Hoffman BM. CO binding to the FeMo cofactor of CO-inhibited nitrogenase: ^{13}CO and ^{1}H Q-band ENDOR investigation. *J Am Chem Soc*. 1997;**119**:10121–6.
49 Lee HI, Hales BJ, Hoffman BM. Metal-ion valencies of the femo cofactor in CO-inhibited and resting state nitrogenase by ^{57}Fe Q-band ENDOR. *J Am Chem Soc*. 1997;**119**:11395–400.
50 Pérez-González A, Yang ZY, Lukoyanov DA, Dean DR, Seefeldt LC, Hoffman BM. Exploring the role of the central carbide of the nitrogenase active-site FeMo-cofactor through targeted ^{13}C labeling and ENDOR spectroscopy. *J Am Chem Soc*. 2021;**143**:9183–90.
51 Buscagan TM, Perez KA, Maggiolo AO, Rees DC, Spatzal T. Structural characterization of two CO molecules bound to the nitrogenase active site. *Angew Chem Int Ed Engl*. 2021;**60**:5704–7.
52 Sippel D, Rohde M, Netzer J, Trncik C, Gies J, Grunau K, et al. A bound reaction intermediate sheds light on the mechanism of nitrogenase. *Science*. 2018;**359**:1484–9.
53 Rohde M, Grunau K, Einsle O. CO binding to the FeV cofactor of CO-reducing vanadium nitrogenase at atomic resolution. *Angew Chem Int Ed Engl*. 2020;**59**:23626–30.
54 Rees JA, Bjornsson R, Kowalska JK, Lima FA, Schlesier J, Sippel D, et al. Comparative electronic structures of nitrogenase FeMoco and FeVco. *Dalton Trans*. 2017;**46**:2445–55.
55 Lee CC, Fay AW, Weng TC, Krest CM, Hedman B, Hodgson KO, et al. Uncoupling binding of substrate CO from turnover by vanadium nitrogenase. *Proc Natl Acad Sci USA*. 2015;**112**:13845–9.
56 Spatzal T, Perez KA, Howard JB, Rees DC. Catalysis-dependent selenium incorporation and migration in the nitrogenase active site iron-molybdenum cofactor. *Elife*. 2015;**4**:1–11.
57 Henthorn JT, Arias RJ, Koroidov S, Kroll T, Sokaras D, Bergmann U, et al. Localized electronic structure of nitrogenase FeMoco revealed by selenium K-edge high resolution X-ray absorption spectroscopy. *J Am Chem Soc*. 2019;**141**:13676–88.
58 Hoeke V, Tociu L, Case DA, Seefeldt LC, Raugei S, Hoffman BM. High-resolution ENDOR spectroscopy combined with quantum chemical calculations reveals the structure of nitrogenase Janus intermediate E4 (4H). *J Am Chem Soc*. 2019;**141**:11984–96.
59 Müller A, Schneider K, Knüttel K, Hagen WR. EPR spectroscopic characterization of an "iron only" nitrogenase S = 3/2 spectrum of component 1 isolated from *Rhodobacter capsulatus*. *FEBS Lett*. 1992;**303**:36–40.
60 Mayhew SG. The redox potential of dithionite and SO2- from equilibrium reactions with flavodoxins, methyl viologen and hydrogen plus hydrogenase. *Eur J Biochem*. 1978;**85**:535–47.
61 Carnahan JE, Mortenson LE, Mower HF, Castle JE. Nitrogen fixation in cell-free extracts of *Clostridium pasteurianum*. *Biochim Biophys Acta*. 1960;**44**:520–35.
62 Tanifuji K, Jasniewski AJ, Villarreal D, Stiebritz MT, Lee CC, Wilcoxen J, et al. Tracing the incorporation of the "ninth sulfur" into the nitrogenase cofactor precursor with selenite and tellurite. *Nat Chem*. 2021;**13**:1228–34.
63 Siegbahn PEM. Structures and energetics for O_2 formation in photosystem II. *Acc Chem Res*. 2009;**42**:1871–80.
64 Siegbahn PEM. Water oxidation mechanism in photosystem II, including oxidations, proton release pathways, O–O bond formation and O_2 release. *Biochim Biophys Acta*. 2013;**1827**:1003–19.
65 Siegbahn PEM. Modeling aspects of mechanisms for reactions catalyzed by metalloenzymes. *J Comput Chem*. 2001;**22**:1634–45.
66 Cao L, Caldararu O, Ryde U. Protonation and reduction of the FeMo cluster in nitrogenase studied by quantum mechanics/molecular mechanics (QM/MM) calculations. *J Chem Theory Comput*. 2018;**14**:6653–78.
67 Dance I. Survey of the geometric and electronic structures of the key hydrogenated forms of FeMo-co, the active site of the enzyme nitrogenase: principles of

the mechanistically significant coordination chemistry. *Inorganics*. 2019;**7**:8.
68 Morrison CN, Hoy JA, Zhang L, Einsle O, Rees DC. Substrate pathways in the nitrogenase MoFe protein by experimental identification of small molecule binding sites. *Biochemistry*. 2015;**54**:2052–60.
69 Igarashi RY, Seefeldt LC. Nitrogen fixation: the mechanism of the Mo-dependent nitrogenase. *Crit Rev Biochem Mol Biol*. 2003;**38**:351–84.
70 Smith D, Danyal K, Raugei S, Seefeldt LC. Substrate channel in nitrogenase revealed by a molecular dynamics approach. *Biochemistry*. 2014;**53**:2278–85.
71 Durrant MC. Controlled protonation of iron–molybdenum cofactor by nitrogenase: a structural and theoretical analysis. *Biochem J*. 2001;**355**:569–76.
72 Barney BM, Yurth MG, Dos Santos PC, Dean DR, Seefeldt LC. A substrate channel in the nitrogenase MoFe protein. *J Biol Inorg Chem*. 2009;**14**:1015–22.
73 Dance I. The controlled relay of multiple protons required at the active site of nitrogenase. *Dalton Trans*. 2012;**41**:7647–59.
74 Dance I. A molecular pathway for the egress of ammonia produced by nitrogenase. *Sci Rep*. 2013;**3**:3237.
75 Dance I. How feasible is the reversible S-dissociation mechanism for the activation of FeMo-co, the catalytic site of nitrogenase? *Dalton Trans*. 2019;**48**:1251–62.
76 Dance I. Ramifications of C-centering rather than N-centering of the active site FeMo-co of the enzyme nitrogenase. *Dalton Trans*. 2012;**41**:4859–65.
77 Siegbahn PEM. Model calculations suggest that the central carbon in the FeMo-cofactor of nitrogenase becomes protonated in the process of nitrogen fixation. *J Am Chem Soc*. 2016;**138**:10485–95.
78 Dance I. New insights into the reaction capabilities of His195 adjacent to the active site of nitrogenase. *J Inorg Biochem*. 2017;**169**:32–43.
79 Dance I. Computational investigations of the chemical mechanism of the enzyme nitrogenase. *Chembiochem*. 2020;**21**:1671–709.
80 Dance I. The pathway for serial proton supply to the active site of nitrogenase: enhanced density functional modeling of the Grotthuss mechanism. *Dalton Trans*. 2015;**44**:18167–86.
81 de Grotthuss CJT. Memoire—Sur la decomposition de l'eau et des corps qu'elle tient en dissolution a l'aide the l'_lectricite galvanique. *Ann Chim*. 1806;**LVIII**:54–74.
82 Dance I. The stereochemistry and dynamics of the introduction of hydrogen atoms onto FeMo-co, the active site of nitrogenase. *Inorg Chem*. 2013;**52**:13068–77.
83 Dance I. Mechanistic significance of the preparatory migration of hydrogen atoms around the FeMo-co active site of nitrogenase. *Biochemistry*. 2006;**45**:6328–40.
84 Schimpl J, Petrilli HM, Blöchl PE. Nitrogen binding to the FeMo-cofactor of nitrogenase. *J Am Chem Soc*. 2003;**125**:15772–8.
85 Kästner J, Hemmen S, Blöchl PE. Activation and protonation of dinitrogen at the FeMo cofactor of nitrogenase. *J Chem Phys*. 2005;**123**:074306.
86 Kästner J, Blöchl PE. Ammonia production at the FeMo cofactor of nitrogenase: results from density functional theory. *J Am Chem Soc*. 2007;**129**:2998–3006.
87 Kästner J, Blöchl PE. Towards an understanding of the workings of nitrogenase from DFT calculations. *ChemPhysChem*. 2005;**6**:1–4.
88 Varley JB, Nørskov JK. First-principles calculations of Fischer–Tropsch processes catalyzed by nitrogenase enzymes. *ChemCatChem*. 2013;**5**:732–6.
89 Varley JB, Wang Y, Chan K, Studt F, Nørskov JK. Mechanistic insights into nitrogen fixation by nitrogenase enzymes. *Phys Chem Chem Phys*. 2015;**17**:29541–7.
90 Rao L, Xu X, Adamo C. Theoretical investigation on the role of the central carbon atom and close protein environment on the nitrogen reduction in Mo nitrogenase. *ACS Catal*. 2016;**6**:1567–77.
91 Dos Santos PC, Igarashi RY, Lee HI, Hoffman BM, Seefeldt LC, Dean DR. Substrate interactions with the nitrogenase active site. *Acc Chem Res*. 2005;**38**:208–14.
92 Dos Santos PC, Mayer SM, Barney BM, Seefeldt LC, Dean DR. Alkyne substrate interaction within the nitrogenase MoFe protein. *J Inorg Biochem*. 2007;**101**:1642–8.
93 Seefeldt LC, Hoffman BM, Dean DR. Mechanism of mo-dependent nitrogenase. *Annu Rev Biochem*. 2009;**78**:701–22.
94 Barney BM, Lee HI, Dos Santos PC, Hoffman BM, Dean DR, Seefeldt LC. Breaking the N_2 triple bond: insights into the nitrogenase mechanism. *Dalton Trans*. 2006;2277–84.
95 Dance I. Mechanisms of the S/CO/Se interchange reactions at FeMo-co, the active site cluster of nitrogenase. *Dalton Trans*. 2016;**45**:14285–300.
96 Dance I. Calculating the chemical mechanism of nitrogenase: new working hypotheses. *Dalton Trans*. 2022;**51**:12717–28.
97 Siegbahn PEM. The mechanism for nitrogenase including all steps. *Phys Chem Chem Phys*. 2019;**21**:15747–59.
98 Siegbahn PEM. Is there computational support for an unprotonated carbon in the E4 state of nitrogenase? *J Comput Chem*. 2018;**39**:743–7.
99 Wei WJ, Siegbahn PEM. A mechanism for nitrogenase including loss of a sulfide. *Chemistry*. 2022;**28**: e202103745.
100 Cao L, Ryde U. Putative reaction mechanism of nitrogenase after dissociation of a sulfide ligand. *J Catal*. 2020;**391**:247–59.

101 Jiang H, Ryde U. Thermodynamically favourable states in the reaction of nitrogenase without dissociation of any sulfide ligand. *Chemistry*. 2022;**28**:35–42.
102 Jiang H, Svensson OKG, Cao L, Ryde U. Proton transfer pathways in nitrogenase with and without dissociated S2B. *Angew Chem Int Ed Engl*. 2022;**61**: e202208544.
103 Cao L, Ryde U. Extremely large differences in DFT energies for nitrogenase models. *Phys Chem Chem Phys*. 2019;**21**:2480–8.
104 Srisantitham S, Badding ED, Suess DLM. Postbiosynthetic modification of a precursor to the nitrogenase iron-molybdenum cofactor. *Proc Natl Acad Sci USA*. 2021;**118**:1–6.
105 Hoffman BM, Roberts JE, Orme-Johnson WH. Mo-95 and H-1 ENDOR spectroscopy of the nitrogenase MoFe protein. *J Am Chem Soc*. 1982;**104**:860–2.
106 Spatzal T, Aksoyoglu M, Zhang L, Andrade SLA, Schleicher E, Weber S, et al. Evidence for interstitial carbon in nitrogenase FeMo cofactor. *Science*. 2011;**334**:940.
107 Hoover TR, Imperial J, Ludden PW, Shah VK. Homocitrate is a component of the iron-molybdenum cofactor of nitrogenase. *Biochemistry*. 1989;**28**:2768–71.
108 Roth LE, Tezcan FA. ATP-uncoupled, six-electron photoreduction of hydrogen cyanide to methane by the molybdenum-iron protein. *J Am Chem Soc*. 2012;**134**:8416–9.
109 Roth LE, Nguyen JC, Tezcan FA. ATP- and iron-protein-independent activation of nitrogenase catalysis by light. *J Am Chem Soc*. 2010;**132**:13672–4.
110 Lee YS, Yuan M, Cai R, Lim K, Minteer SD. Nitrogenase bioelectrocatalysis: ATP-independent ammonia production using a redox polymer/MoFe protein system. *ACS Catal*. 2020;**10**:6854–61.
111 Lee YS, Ruff A, Cai R, Lim K, Schuhmann W, Minteer SD. Electroenzymatic nitrogen fixation using a MoFe protein system immobilized in an organic redox polymer. *Angew Chem Int Ed Engl*. 2020;**59**:16511–6.
112 Wenke BB. The many roles of the nitrogenase iron protein. Thesis. California Institute of Technology; 2019.
113 Warmack RA, Rees DC. Anaerobic single particle cryoEM of nitrogenase. *bioRxiv*. 2022. https://doi.org/10.1101/2022.06.04.494841
114 Rutledge HL, Cook BD, Nguyen HPM, Herzik MA, Tezcan FA. Structures of the nitrogenase complex prepared under catalytic turnover conditions. *Science*. 2022;**377**:865–9.
115 Li Z, Li J, Dattani NS, Umrigar CJ, Chan GKL. The electronic complexity of the ground-state of the FeMo cofactor of nitrogenase as relevant to quantum simulations. *J Chem Phys*. 2019;**150**:024302.
116 Li Z, Guo S, Sun Q, Chan GK-L. The electronic landscape of the P-cluster of nitrogenase. *Nat Chem*. 2019;**11**:1026–33.
117 McSkimming A, Suess DLM. Dinitrogen binding and activation at a molybdenum–iron–sulfur cluster. *Nat Chem*. 2021;**13**:666–70.
118 Ohki Y, Munakata K, Matsuoka Y, Hara R, Kachi M, Uchida K, et al. Nitrogen reduction by the Fe sites of synthetic [Mo3S4Fe] cubes. *Nature*. 2022;**607**:86–90.